Regulation of systolic $[Ca^{2+}]_i$ and cellular Ca^{2+} flux balance in rat ventricular myocytes by SR Ca^{2+}, L-type Ca^{2+} current and diastolic $[Ca^{2+}]_i$

K. M. Dibb, D. A. Eisner and A. W. Trafford

Unit of Cardiac Physiology, University of Manchester, Core Technology Facility, 46 Grafton Street, Manchester M13 9NT, UK

The force–frequency response is an important physiological mechanism regulating cardiac output changes and is accompanied *in vivo* by β-adrenergic stimulation. We sought to determine the role of sarcoplasmic reticulum (SR) Ca^{2+} content and L-type current ($I_{Ca\text{-}L}$) in the frequency response of the systolic Ca^{2+} transient alone and during β-adrenergic stimulation. Experiments (on single rat ventricular myocytes) were designed to be as physiological as possible. Under current clamp stimulation SR Ca^{2+} content increased in line with stimulation frequency (1–8 Hz) but the systolic Ca^{2+} transient was maximal at 6 Hz. Under voltage clamp, increasing frequency decreased both systolic Ca^{2+} transient and $I_{Ca\text{-}L}$. Normalizing peak $I_{Ca\text{-}L}$ by altering the test potential decreased the Ca^{2+} transient amplitude less than an equivalent reduction achieved through changes in frequency. This suggests that, in addition to SR Ca^{2+} content and $I_{Ca\text{-}L}$, another factor, possibly refractoriness of Ca^{2+} release from the SR contributes. Under current clamp, β-adrenergic stimulation (isoprenaline, 30 nM) increased both the Ca^{2+} transient and the SR Ca^{2+} content and removed the dependence of both on frequency. In voltage clamp experiments, β-adrenergic stimulation still increased SR Ca^{2+} content yet there was an inverse relation between frequency and Ca^{2+} transient amplitude and $I_{Ca\text{-}L}$. Diastolic $[Ca^{2+}]_i$ increased with stimulation frequency and this contributed substantially (69.3 $\pm$ 6% at 8 Hz) to the total Ca^{2+} efflux from the cell. We conclude that Ca^{2+} flux balance is maintained by the combination of increased efflux due to elevated diastolic $[Ca^{2+}]_i$ and a decrease of influx on $I_{Ca\text{-}L}$ on each pulse.

(Received 25 July 2007; accepted after revision 5 October 2007; first published online 11 October 2007)
Corresponding author K. M. Dibb: Unit of Cardiac Physiology, University of Manchester, Core Technology Facility, 46 Grafton Street, Manchester M13 9NT, UK. Email: katharine.dibb@manchester.ac.uk

In cardiac muscle changes in stimulation frequency alter the force of contraction. This so-called 'force–frequency' response is an important mechanism by which cardiac output changes to meet the varying metabolic demands of the body. The force–frequency response is also observed in isolated cardiac myocytes and is accompanied by a frequency-dependent acceleration of the rate of decay of the systolic Ca^{2+} transient (Hussain *et al.* 1997). The nature of the force–frequency response varies between studies with some reporting a positive (Janssen *et al.* 2002; Antoons *et al.* 2002), some a negative (Bouchard & Bose, 1989; Maier *et al.* 2000) and even some showing both positive and negative staircases (Layland & Kentish, 1999; Kassiri *et al.* 2000). There are several potential mechanisms underlying these disparate results: (i) the use of stimulation rates that are non-physiological for the species concerned, (ii) ranges in experimental temperature between 23 and 37.5°C, and (iii) the species used.

Most of the Ca^{2+} required for the activation of contraction is released from the sarcoplasmic reticulum (SR) in response to Ca^{2+} entering the cell via $I_{Ca\text{-}L}$ during the action potential. Both the SR Ca^{2+} content and $I_{Ca\text{-}L}$ regulate the amplitude of the systolic Ca^{2+} transient (Bassani *et al.* 1995; Trafford *et al.* 2000, 2001). Additionally, with changes in stimulation frequency it is reported that, depending on the experimental conditions, $I_{Ca\text{-}L}$ can be either increased (facilitated) (Guo & Duff, 2003; Picht *et al.* 2007) or reduced (Antoons *et al.* 2002), and thus also potentially contributing to the mixed reports above. Furthermore, *in vivo* increases in heart rate are due to increased β-adrenergic stimulation. β-Adrenergic stimulation results in the phosphorylation of key cellular proteins involved in regulating $[Ca^{2+}]_i$, e.g. $I_{Ca\text{-}L}$ and phospholamban, and thus the activity of the SR Ca^{2+}-ATPase (see Bers, 2001 for review). However, how such β-adrenergic stimulation modulates

 DOI: 10.1113/jphysiol.2007.141473

the frequency-dependent response of isolated cardiac myocytes remains unclear particularly at physiologically relevant rates of stimulation and temperature. Another important question concerns how Ca^{2+} flux balance is maintained at increased frequencies since each action potential results in Ca^{2+} entry into the cell via $I_{Ca\text{-}L}$ and therefore one might expect increased influx per unit time at higher frequencies.

The aims of this work were therefore to determine: (i) the mechanisms responsible for the frequency-dependent changes in Ca^{2+} transient amplitude and how these are altered by β-adrenergic stimulation, and (ii) how cellular Ca^{2+} flux balance is maintained as stimulation frequency is elevated. We have used conditions designed to be as physiologically relevant as possible (stimulation rates, temperature, current clamp and perforated patch to minimize intracellular dialysis). The main findings are that SR Ca^{2+} content increases with stimulation rate yet Ca^{2+} transient amplitude shows a biphasic (increasing and then decreasing) response. Changes in $I_{Ca\text{-}L}$ are involved but do not fully explain the dissociation between SR Ca^{2+} content and Ca^{2+} transient amplitude. β-Adrenergic stimulation flattens both the frequency–Ca^{2+} transient amplitude and frequency–SR Ca^{2+} content relationships. Finally, Ca^{2+} flux balance is maintained by a combination of decreased Ca^{2+} entry per pulse and an increase of diastolic $[Ca^{2+}]_i$.

Methods

All experiments accord with the United Kingdom Animals (Scientific Procedures) Act 1986.

Cell isolation and $[Ca^{2+}]_i$ measurements

Rats were killed by stunning and cervical dislocation, and single ventricular myocytes were isolated using an enzymatic digestion process as previously described (Trafford *et al.* 1997). Changes in intracellular Ca^{2+} concentration ($[Ca^{2+}]_i$) were measured using Fluo-3 AM as previously described (Dibb *et al.* 2004). Briefly, myocytes were loaded with 5 μM Fluo-3 AM for 5 min at room temperature before resuspension in a modified Tyrode solution containing (mM): NaCl, 134; glucose, 11.1; Hepes, 10; KCl, 4; $MgCl_2$, 1.2; $CaCl_2$, 1 and titrated to pH 7.35 using NaOH. Myocytes were left for at least 30 min for the indicator to de-esterify prior to experimentation. Fluorescence was excited at 488 nm and emitted light (> 520 nm) converted to $[Ca^{2+}]_i$ assuming a K_d of 864 nm (Ito *et al.* 2000). The rates of decay of the systolic and caffeine evoked Ca^{2+} transients were obtained by fitting single exponential functions to the decay phase of the transient. In each cell the decay curve was fitted over the same range of $[Ca^{2+}]_i$. All experiments were performed at $37 \pm 0.1^{\circ}$C using a heat superfusion system (Cell Micro-Controls, Norfolk, VA, USA).

Cell electrophysiology and SR Ca^{2+} content measurements

All experiments were performed using the perforated patch clamp technique under current- or voltage-clamp control (using switch-clamp compensation for series resistance errors) using the AxoClamp 2B voltage clamp amplifier (Axon Instruments, Union City, CA, USA) as previously described (Dibb *et al.* 2004). Micropipettes (< 2 MΩ) were filled with (mM): KCH_3O_3S, 125; KCl, 20; NaCl, 10; Hepes, 10; $MgCl_2$, 5; titrated to pH 7.2 with KOH and amphotericin-B (final concentration 240 μg ml^{-1}). Myocytes were stimulated to elicit action potentials (current clamp) or $I_{Ca\text{-}L}$ (voltage clamp) over a range of frequencies (1–8 Hz) encompassing the physiological range for the rat. Isoprenaline (30 nM) was used to investigate the effects of β-adrenergic stimulation.

SR Ca^{2+} content was assessed following trains of action potentials by rapidly switching to voltage clamp control at a holding potential of −80 mV and applying 10 mM caffeine to discharge SR Ca^{2+}. The resultant Na^+–Ca^{2+} exchanger current was integrated and corrected for Ca^{2+} removal by non-electrogenic mechanisms as previously described (Varro *et al.* 1993).

Frequency-dependent effects on $I_{Ca\text{-}L}$ were investigated under voltage clamp control using a holding potential of either −40 mV or −80 mV and a 50 ms test pulse to 0 mV at the above range of frequencies. In some experiments where a holding potential of −80 mV was used (Figs 5, 6 and 7), 30 μM tetrodotoxin (TTX) was added to the superfusate to block the fast sodium current.

The SR-dependent rate of Ca^{2+} uptake (k_{SR}) was calculated by subtracting the rate of decay of the caffeine evoked Ca^{2+} transient (k_{caff}, e.g. Fig. 2*B*, where SR mediated Ca^{2+} uptake is effectively inhibited) from the rate of decay of the systolic Ca^{2+} transient (k_{sys}, where SR and sarcolemmal Ca^{2+} efflux are active) (Díaz *et al.* 2004).

Statistics

All data are presented as mean ± standard error of the mean (S.E.M.) for n experiments. Tests for differences were performed using repeated measures analysis of variance with a suitable *post hoc* test or Student's t test where appropriate. $P < 0.05$ was considered significant.

Results

Frequency dependence of the systolic Ca^{2+} transient

The results of a typical experiment are illustrated in Fig. 1*A*. At physiological rates of stimulation for the rat (4–8 Hz), diastolic $[Ca^{2+}]_i$ increases with frequency (Fig. 1*B*, 4 Hz, 155 ± 25 nM; 6 Hz, 202 ± 31 nM; 8 Hz, 255 ± 39 nM; $n = 11$–14 cells, $P < 0.001$). However, the amplitude of the systolic Ca^{2+} transient is greatest at 6 Hz (Fig. 1*B*, 4 Hz, 244 ± 21 nM; 6 Hz, 319 ± 28 nM; 8 Hz,

279 ± 27 nM; $P < 0.01$ for 4 and 8 Hz *versus* 6 Hz and $P < 0.05$ for 4 Hz *versus* 8 Hz). Thus under physiological conditions of temperature and frequency the amplitude of the Ca^{2+} transient does not simply increase with stimulation frequency. Changes in action potential duration are examined in Fig. 1*C* and *D*. Whilst the time to 90% repolarization increases between 4 and 6 Hz with the larger Ca^{2+} transient amplitude (51.7 ± 3 *versus* 62.8 ± 5 ms, $P < 0.05$) there is no further change in action potential duration at 8 Hz (59.1 ± 8 ms). Given that action potential duration was unchanged between 6 and 8 Hz other factors must underlie the decrease in Ca^{2+} transient amplitude between these frequencies. In the next sections we investigate whether changes of SR Ca content or $I_{Ca\text{-}L}$ contribute.

A role for enhanced SERCA function and SR Ca^{2+} content?

Figure 1*E* shows normalized systolic Ca^{2+} transients. With increasing stimulation frequency the rate of decay of $[Ca^{2+}]_i$ accelerates (4 Hz, 13.7 ± 0.6 s^{-1}; 6 Hz, 20.8 ± 0.9 s^{-1}; 8 Hz, 24.2 ± 1.4 s^{-1}; $P < 0.01$, Fig. 1*F*). Given that SERCA is the primary route for Ca^{2+} removal this accelerated rate of decay is indicative of enhanced SERCA function and indeed k_{SR} (the SR dependent rate constant) increases with stimulation frequency (4 Hz, 11.1 ± 0.9 s^{-1}; 6 Hz, 16.6 ± 0.8 s^{-1}; 8 Hz, 19.5 ± 1.5 s^{-1}; $P < 0.05$, Fig. 1*G*).

Figure 2*A* illustrates the experimental protocol to determine SR Ca^{2+} content following current clamp stimulation. After a switch to voltage clamp control 10 mM caffeine was rapidly applied to the cell to discharge SR Ca^{2+} (Fig. 2*B*). SR Ca^{2+} content increased with stimulation frequency (4 Hz, 69.2 ± 5 μmol l^{-1}; 6 Hz, 94.2 ± 7 μmol l^{-1}; 8 Hz, 110 ± 7 μmol l^{-1}; $P < 0.05$, $n = 12$ cells, Fig. 2*C*). Figure 2*D* examines the relationship between $[Ca^{2+}]_i$ and Na^+–Ca^{2+} exchange current obtained during the decay phase of the caffeine evoked Ca^{2+} transient when $[Ca^{2+}]_i$ and Na^+–Ca^{2+} exchange current are in equilibrium (Trafford *et al.* 1998). The data have been fitted with linear regressions, the slopes of which

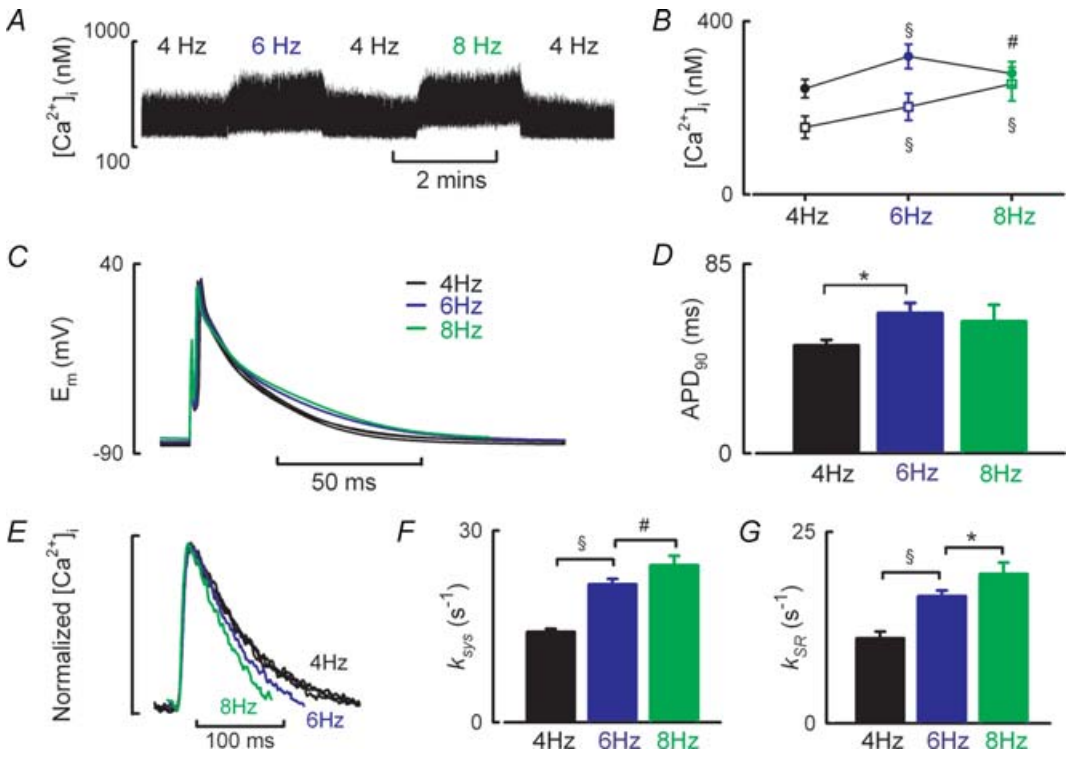

Figure 1. Frequency dependence of the systolic Ca^{2+} transient, action potential duration and SR function during current clamp stimulation

A, slow time course of a typical experiment showing the effects of stimulation rate on $[Ca^{2+}]_i$. Action potentials were initiated at the frequencies indicated by a 2–4 ms depolarizing current pulse. *B*, mean data summarizing the frequency dependence of diastolic $[Ca^{2+}]_i$ (open symbols) and Ca^{2+} transient amplitude (filled symbols). *C*, representative action potentials obtained at the stimulation frequencies indicated. *D*, mean data summarizing time to 90% repolarization of the action potential. *E*, normalized Ca^{2+} transients illustrating frequency-dependent acceleration of $[Ca^{2+}]_i$ decay. *F*, mean data summarizing rate decay constant of the systolic Ca^{2+} transient. *G*, mean data summarizing the SR dependent rate of Ca^{2+} removal. *$P < 0.05$, #$P < 0.01$ and §$P < 0.001$.

do not change with stimulation frequency indicating that Na^+–Ca^{2+} exchanger function does not change under these conditions (4 Hz, -0.186 pA nM^{-1}; 6 Hz, -0.192 pA nM^{-1}; 8 Hz, -0.184 pA nM^{-1}). Taken together the increased SR Ca^{2+} content, enhanced SERCA mediated Ca^{2+} uptake rate and unaltered relationship between $[Ca^{2+}]_i$ and Na^+–Ca^{2+} exchange current are consistent with an increase in SERCA function being responsible for the frequency dependent acceleration of the systolic Ca^{2+} transient. However, it is clear from the data of Figs 1 and 2 that changes in $[Ca^{2+}]_i$ with stimulation frequency do *not* follow those of SR Ca^{2+} content.

The effects of frequency under voltage clamp conditions

In the next series of experiments we used voltage clamp stimulation since (i) this eliminates any effects due to changes of action potential duration, and (ii) it makes it possible to evaluate the role of changes of $I_{Ca\text{-}L}$. Figure 3*A* shows a typical experimental record for this type of experiment. A baseline frequency of 1 Hz was chosen in these experiments in order to allow the effects of recovery of $I_{Ca\text{-}L}$ from inactivation to be studied. Figure 3*B* shows representative Ca^{2+} transients and summarizes the mean data for changes in diastolic $[Ca^{2+}]_i$ and Ca^{2+} transient amplitude. Under these voltage clamp conditions (holding potential of -40 mV, 50 ms duration step to 0 mV) diastolic $[Ca^{2+}]_i$ increases with stimulation frequency (1 Hz, 120 ± 11 nM; 4 Hz, 133 ± 11 nM; 6 Hz, 156 ± 13 nM; 8 Hz, 179 ± 18 nM. $P < 0.05$, $n = 9$–10 cells, centre panel) whereas (in contrast to the current clamp data of Fig. 1) the amplitude of the systolic Ca^{2+} transient decreased (1 Hz, 263 ± 30 nM; 4 Hz, 217 ± 30 nM; 6 Hz, 153 ± 23 nM; 8 Hz, 87 ± 17 nM. $P < 0.01$, lower panel). The frequency-dependent decrease in Ca^{2+} transient amplitude was mirrored by reductions in peak $I_{Ca\text{-}L}$. Figure 3*C* shows representative current records and summarizes the mean data for peak $I_{Ca\text{-}L}$ density and rate of inactivation of $I_{Ca\text{-}L}$. Peak $I_{Ca\text{-}L}$

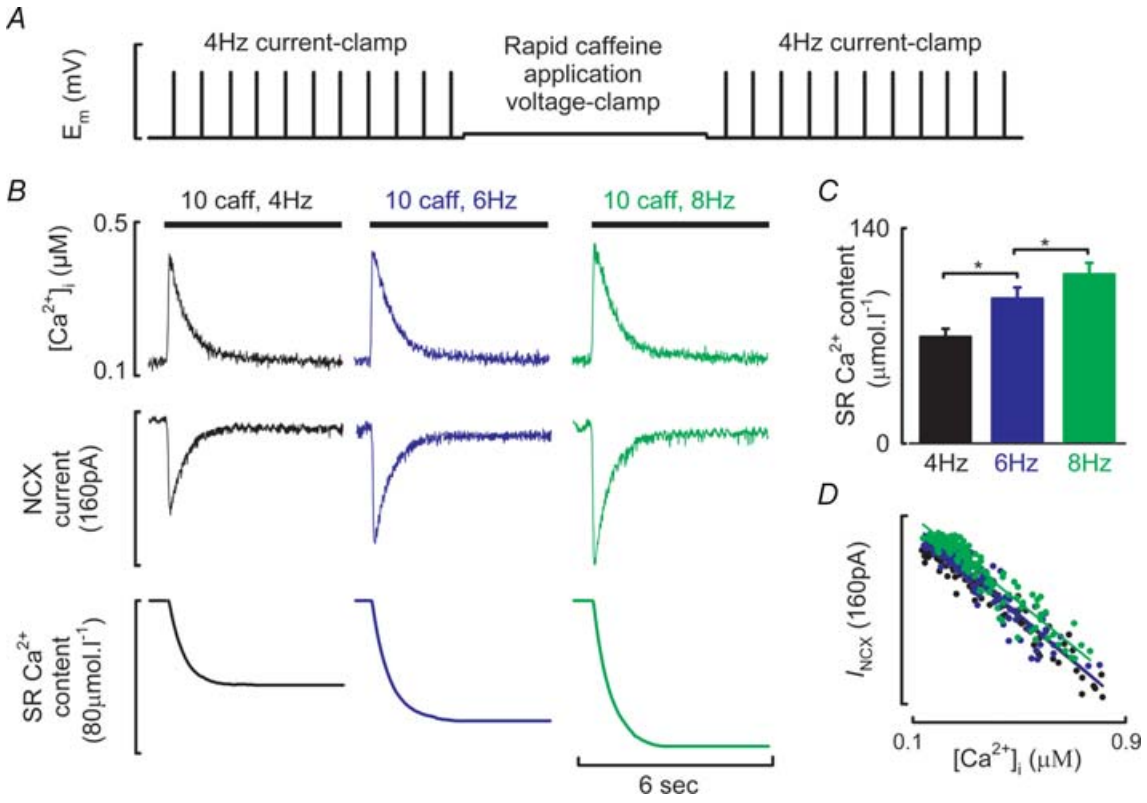

Figure 2. Modulation of SR Ca^{2+} content by stimulation frequency
A, schematic of the experimental protocol used to quantify SR Ca^{2+} content following current clamp stimulation. *B*, quantification of SR Ca^{2+} content following steady state stimulation at the frequencies indicated. Caffeine at 10 mM was applied for the time indicated by the filled bars resulting in a caffeine evoked Ca^{2+} transient (top), inward Na^+–Ca^{2+} exchange current (centre) which when integrated gives a quantitative measure of SR Ca^{2+} content (lower). *C*, mean data summarizing SR Ca^{2+} contents at the stimulation frequencies indicated. *D*, Na^+–Ca^{2+} exchange current as a function of $[Ca^{2+}]_i$ obtained during the decay phase of the caffeine evoked Ca^{2+} transient. 4 Hz, black; 6 Hz, blue; 8 Hz, green. $^*P < 0.05$.

density is inversely related to stimulation frequency (1 Hz, 7.45 ± 0.9 pA pF^{-1}; 4 Hz, 5.18 ± 0.7 pA pF^{-1}; 6 Hz, 3.66 ± 0.5 pA pF^{-1}; 8 Hz, 2.36 ± 0.3 pA pF^{-1}; $P < 0.05$, centre panel) whilst the time constant of inactivation of $I_{Ca\text{-}L}$ increased with rate (1 Hz, 8.77 ± 0.6 ms; 4 Hz, 9.45 ± 0.6 ms; 6 Hz, 10.6 ± 0.7 ms; 8 Hz, 12.2 ± 0.8 ms; $P < 0.05$, lower panel).

In contrast to the opposite effects of frequency on the amplitude of the Ca^{2+} transient between current clamp and voltage clamp, other parameters were not greatly different with the two methods of stimulation. Thus increasing stimulation frequency still increased the rate constant of decay of the systolic Ca^{2+} transient (data not shown) and SR Ca^{2+} content increased with stimulation frequency between 1 and 6 Hz although there was no significant change between 6 and 8 Hz (1 Hz, 79.6 ± 8; 4 Hz, 86.9 ± 7; 6 Hz; 94.1 ± 8; Fig. 3*B* lower panel).

The above data raise two important questions: (i) is the decrease of the systolic Ca^{2+} transient caused by the observed decrease of the amplitude of $I_{Ca\text{-}L}$? (ii) Is the decrease of $I_{Ca\text{-}L}$ with increased frequency due to the depolarized (−40 mV) membrane potential used in these experiments? We will consider these in turn.

Do changes in $I_{Ca\text{-}L}$ fully explain the frequency–systolic $[Ca^{2+}]_i$ relationship?

The next series of experiments was designed to determine if the reduction in peak $I_{Ca\text{-}L}$ is responsible for the change in Ca^{2+} transient amplitude. In these experiments the effects of increasing frequency were compared with those of decreasing peak $I_{Ca\text{-}L}$ by reducing the amplitude of the voltage clamp test step. Figure 4*A* illustrates the result of a typical experiment. During voltage clamp stimulation (1 Hz with 50 ms duration pulses from a holding potential of −40 to 0 mV) reducing the test step from 0 mV to −15 mV resulted in an immediate large decrease in peak $I_{Ca\text{-}L}$ from 314 to 76 pA accompanied by a more modest reduction in the amplitude of the Ca^{2+} transient (from 64 to 43 nM). Figure 4*B* shows the

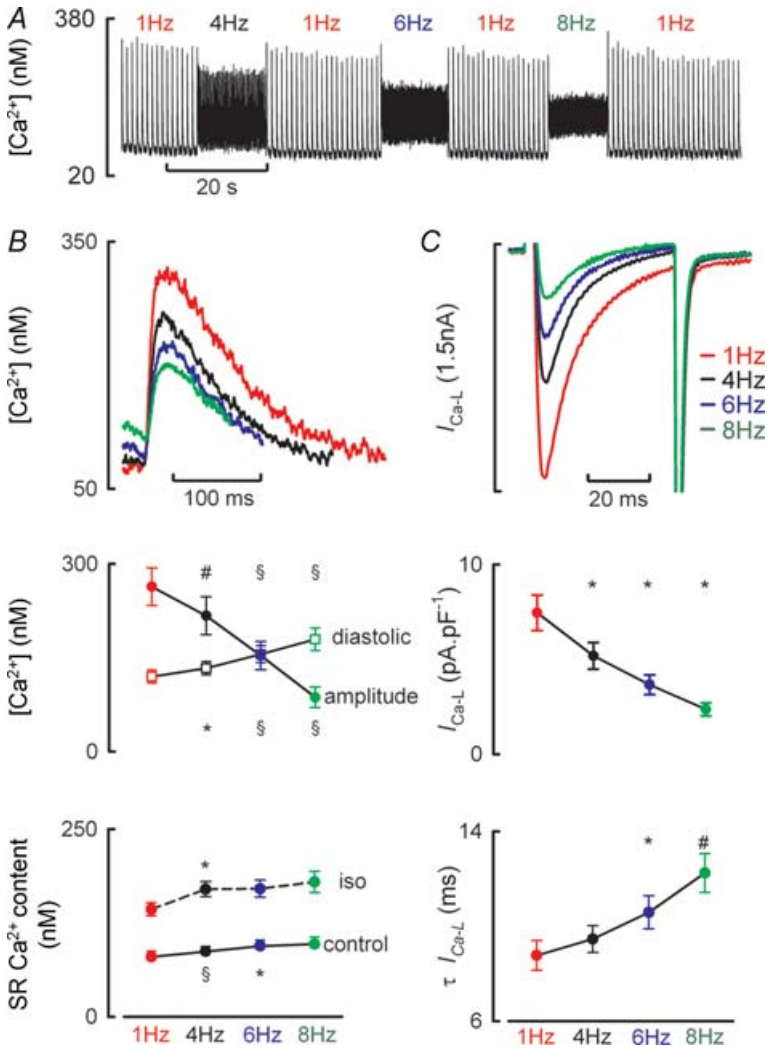

Figure 3. The frequency–$[Ca^{2+}]_i$ relationship is altered under voltage clamp conditions
A, experimental time course showing typical relationship between $[Ca^{2+}]_i$ and stimulation frequency in a voltage clamped myocyte. Cells were stimulated with 50 ms depolarizing step to 0 mV from a holding potential of −40 mV at the frequencies indicated. *B*, upper, typical systolic Ca^{2+} transients obtained at the frequencies indicated; centre, mean data summarizing Ca^{2+} transient amplitude (filled symbols) and diastolic $[Ca^{2+}]_i$ (open symbols); lower, SR Ca^{2+} content in control and isoprenaline. *C*, top, membrane current records for the same Ca^{2+} transients shown in *B*; centre, mean data summarizing peak inward $I_{Ca\text{-}L}$; lower, time constant of $I_{Ca\text{-}L}$ inactivation. $^*P < 0.05$, #$P < 0.01$ and §$P < 0.001$ when compared to previous frequency.

results from similar experiments obtained during superfusion with either control solution or in the presence of 30 nM isoprenaline. Decreases in $I_{Ca\text{-}L}$ brought about by changes in stimulation frequency either in control (filled black circles) or β-adrenergic stimulation (filled pink triangles) result in a decrease in Ca^{2+} transient amplitude.

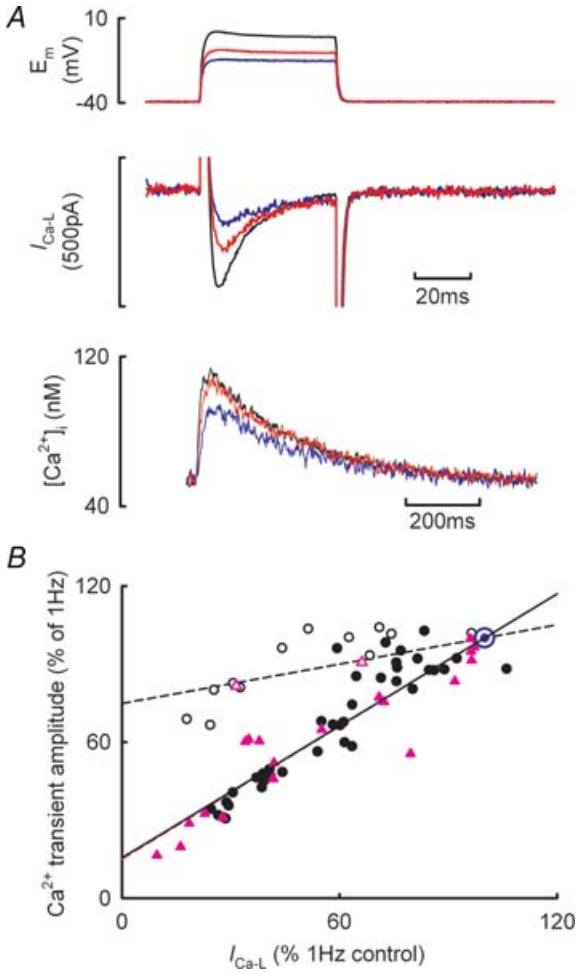

Figure 4. Frequency-dependent reductions in $I_{Ca\text{-}L}$ are not entirely responsible for the decrease in Ca^{2+} transient amplitude with increased stimulation rate
A, typical experimental traces for membrane potential (top), membrane current (centre) and $[Ca^{2+}]_i$ (bottom). Records obtained from a holding potential of −40 mV and test steps to 0 mV (black), −10 mV (red) and −15 mV (blue). *B*, dependence of Ca^{2+} transient amplitude on peak $I_{Ca\text{-}L}$. Data have been normalized to the respective values at 1 Hz. Filled symbols show data obtained by changing stimulation frequency either in control solutions (black circles) or during β-adrenergic stimulation (pink triangles). Open symbols show data obtained by changing $I_{Ca\text{-}L}$ through alteration of the amplitude of the voltage clamp step either in control (circles) or during β-adrenergic stimulation (triangles). The lines through the data are best fit linear regressions forced through $x = 100$, $y = 100$ (blue symbol) and show fits to the control frequency data (continuous black line), β-adrenergic stimulation frequency data (broken pink line, having identical slope and intercept to control data) and the altered test step amplitude data (broken black line, control data only).

In both conditions the relationship between Ca^{2+} transient amplitude (ordinate) and peak $I_{Ca\text{-}L}$ (abscissa) is linear having the same slope (control, 0.844 ± 0.03; β-adrenergic stimulation, 0.849 ± 0.04). However, abruptly reducing peak $I_{Ca\text{-}L}$ by decreasing the amplitude of the test step results in a smaller decrease in Ca^{2+} transient amplitude (open symbols). When the test step amplitude is reduced the slope of the relationship between Ca^{2+} transient amplitude and peak $I_{Ca\text{-}L}$ is now 0.252 ± 0.04 ($P < 0.02$ compared to both the control and β-adrenergic stimulation frequency responses). These data therefore demonstrate that under voltage clamp conditions, most of the reduction in Ca^{2+} transient amplitude with increasing stimulation frequency is *not* due to the decrease in peak $I_{Ca\text{-}L}$.

Effect of holding potential on $I_{Ca\text{-}L}$ and the systolic Ca^{2+} transient

The observed decrease in $I_{Ca\text{-}L}$ with stimulation frequency (Fig. 3) may be due to incomplete recovery of $I_{Ca\text{-}L}$ from inactivation. Recovery from voltage-dependent inactivation is facilitated at more negative membrane potentials and therefore the results described in Fig. 3 (holding potential of −40 mV) may not accurately reflect the results observed under current clamp conditions where resting membrane potential is close to −80 mV (-78.7 ± 0.7 mV at 4 Hz, $n = 13$ cells).

Figure 5 examines the influence of holding potential on the frequency-dependent changes in $I_{Ca\text{-}L}$. Figure 5*A* shows a representative experimental time course for $[Ca^{2+}]_i$ during 50 ms depolarizing pulses to 0 mV from holding potentials of −40 mV and −80 mV and at −80 mV in the presence of isoprenaline. TTX was present throughout these experiments to block I_{Na}. Figure 5*B* shows $I_{Ca\text{-}L}$ and $[Ca^{2+}]_i$ records under the same experimental conditions as above. Compared to when a holding potential of −40 mV is used it is clear that (i) peak $I_{Ca\text{-}L}$ is greater at all frequencies, (ii) peak $I_{Ca\text{-}L}$ decreases to a smaller extent with frequency, and (iii) there is a much greater increase in diastolic $[Ca^{2+}]_i$ with frequency at the more negative holding potential of −80 mV. Figure 5*C*–*E* summarizes the mean data for peak $I_{Ca\text{-}L}$, diastolic $[Ca^{2+}]_i$ and Ca^{2+} transient amplitude in these experiments. For the peak $I_{Ca\text{-}L}$ and Ca^{2+} transient amplitude measurements the data have been normalized to the respective value at 1 Hz and appropriate holding potential. Following stimulation at 8 Hz, peak $I_{Ca\text{-}L}$ decreases to $28 \pm 0.8\%$ and $65 \pm 2.5\%$ of the 1 Hz values at holding potentials of −40 mV and −80 mV, respectively ($P < 0.001$ compared to 1 Hz, $n = 4$–7, Fig. 5*C*). However, the frequency-dependent decrease in Ca^{2+} transient amplitude is substantially attenuated at the more negative holding potential. At a stimulation frequency of 8 Hz, Ca^{2+} transient amplitude

decreases to $34.5 \pm 1.4\%$ and $85.1 \pm 4.4\%$ of the 1 Hz values at −40 and −80 mV, respectively ($P < 0.001$, Fig. 5*E*). It is also clear from Fig. 5*D* that whilst diastolic $[Ca^{2+}]_i$ is identical at 1 Hz at both holding potentials (63 ± 4 and 63 ± 3 nM at −40 and −80 mV, respectively), there is a far greater increase in diastolic $[Ca^{2+}]_i$ with stimulation frequency at −80 mV (113 ± 8 and 179 ± 31 nM at 8 Hz at −40 and −80 mV, respectively, $P < 0.001$).

The above data showing that diastolic $[Ca^{2+}]_i$ increases with stimulation frequency suggest that the interstimulus interval is important in allowing sufficient time for the Ca^{2+} transient to decay. However, this cannot be the only explanation given the greater increase in diastolic $[Ca^{2+}]_i$ with frequency when a more negative holding potential is used. One possible mechanism is the increased trans-sarcolemmal Ca^{2+} entry at −80 mV. With holding potentials of both −40 and −80 mV the Ca^{2+} entry per pulse on $I_{Ca\text{-}L}$ decreases with increasing frequency. However, the Ca^{2+} entry *per unit time* behaves differently depending on the holding potential. Integration of $I_{Ca\text{-}L}$ obtained at a holding potential of −40 mV shows that whilst Ca^{2+} entry increases between 1 and 4 Hz there is no further change in Ca^{2+} entry at higher frequencies (1 Hz, 2.1 ± 0.2 μmol l^{-1} s^{-1}; 4 Hz, 4.5 ± 0.6 μmol l^{-1} s^{-1}; 6 Hz, 5.0 ± 0.3 μmol l^{-1} s^{-1}; 8 Hz, 5.3 ± 0.5 μmol l^{-1} s^{-1}; $P < 0.001$ between 1 and 4 Hz). Conversely, when the more negative (−80 mV) holding potential is used, not only is the integrated Ca^{2+} entry greater at each frequency when compared to the equivalent value obtained at a holding potential of −40 mV ($P < 0.001$), it also increases with stimulation frequency (1 Hz, 3.2 ± 0.2 μmol l^{-1} s^{-1}; 4 Hz, 11.0 ± 0.5 μmol l^{-1} s^{-1}; 6 Hz, 14.3 ± 0.9 μmol l^{-1} s^{-1}; 8 Hz, 17.2 ± 1.3 μmol l^{-1} s^{-1}; $P < 0.001$ between frequencies).

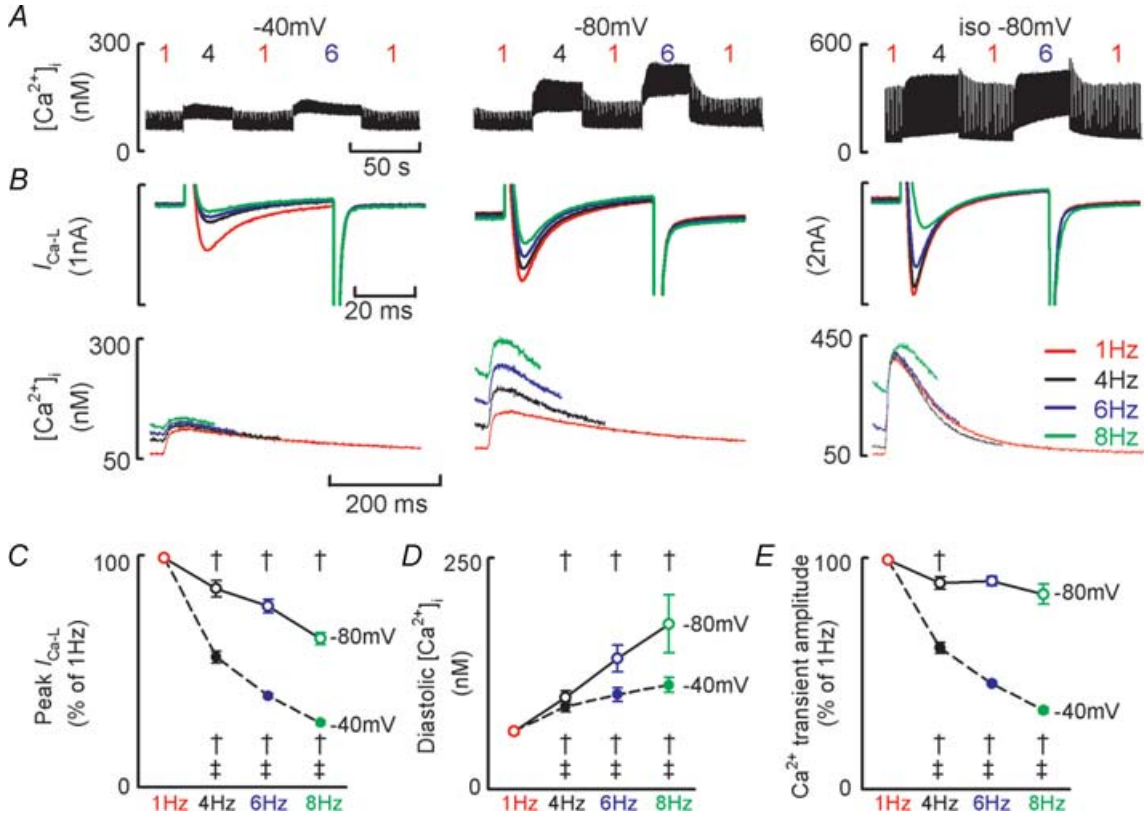

Figure 5. Holding potential influences the frequency dependence of $I_{Ca\text{-}L}$ recovery from inactivation and the frequency dependence of the systolic Ca^{2+} transient

A, representative experimental time courses. Test steps of 50 ms to 0 mV were applied at the frequencies indicated from a holding potential of −40 mV (left) or −80 mV (middle) and at −80 mV in isoprenaline (right). *B*, sample $I_{Ca\text{-}L}$ records (upper) and Ca^{2+} transients (lower) obtained from a holding potential of −40 mV (left), −80 mV (middle) and −80 mV in isoprenaline (right). For *A* and *B* note different ordinate scales used for isoprenaline data. For *A* and *B* all data obtained from the same cell. *C*, mean data summarizing change in peak $I_{Ca\text{-}L}$ with stimulation frequency. *D*, mean data summarizing change in diastolic $[Ca^{2+}]_i$. *E*, mean data summarizing Ca^{2+} transient amplitude. For panels *C* and *E* data have been normalized to the respective value obtained at 1 Hz. Filled symbols denote data obtained from −40 mV holding potential. Open symbols denote data obtained from −80 mV holding potential. †$P < 0.05$ compared to the previous frequency at the same holding potential; ‡$P < 0.05$ comparing the same frequency at each holding potential.

Influence of diastolic $[Ca^{2+}]_i$ in setting cellular Ca^{2+} flux balance

In order for steady state conditions to prevail, the amount of Ca^{2+} entering the cell during the action potential, primarily via $I_{Ca\text{-}L}$, must be balanced by a similar efflux from the cell occurring largely through the Na^+–Ca^{2+} exchanger. This Ca^{2+} efflux can occur either during the systolic Ca^{2+} transient or by increasing diastolic $[Ca^{2+}]_i$ (Trafford *et al.* 1997; Eisner *et al.* 1998). The most striking aspect of the data presented in Fig. 5 is the increase in diastolic $[Ca^{2+}]_i$ with frequency when a resting membrane potential of −80 mV is used. Figure 6 examines the role of the increase in diastolic $[Ca^{2+}]_i$ in ensuring that Ca^{2+} flux balance is maintained. Typical Ca^{2+} transients obtained from the same cell stimulated at 1 Hz and 4 Hz are shown in Fig. 6*A* (holding potential −80 mV, 50 ms step to 0 mV). The shaded areas represent, respectively, the area under the systolic Ca^{2+} transient (yellow hatching) and the area under the Ca^{2+} transient due to the increase in diastolic $[Ca^{2+}]_i$ referenced to the diastolic $[Ca^{2+}]_i$ at 1 Hz (cyan hatching). If we assume that Na^+–Ca^{2+} exchange activity is proportional to $[Ca^{2+}]_i$, then the amount of Ca^{2+} pumped out of the cell (above resting or basal levels) will be proportional to the increase of $[Ca^{2+}]_i$ above resting levels (i.e. the diastolic $[Ca^{2+}]_i$ reached at the slowest rate of stimulation when diastolic $[Ca^{2+}]_i$ is stable between stimuli). Therefore, at 1 Hz the efflux per pulse will be proportional to the integral of the systolic Ca^{2+} transient (the yellow hatched area of Fig. 6*A*). At higher frequencies, e.g. 4 Hz in right hand panel of Fig. 6*A*, the efflux will be proportional to the sum of the systolic (yellow hatched) and diastolic (cyan hatched) integrals. The constant of proportionality will depend on the properties of Na^+–Ca^{2+} exchange and in particular (since the Na^+–Ca^{2+} exchanger is voltage dependent) on the holding potential. Figure 6*B*, left panel examines the relationship between Ca^{2+} entry via $I_{Ca\text{-}L}$ and Ca^{2+} efflux calculated as the integral of the systolic Ca^{2+} transient for data obtained at holding potentials of −40 and −80 mV. Here, the open symbols represent the mean data obtained at 1 Hz (−40 mV, black; −80 mV, red) and have been fitted with linear regressions passing through the origin having slopes 9.13 ± 0.8 and 7.25 ± 0.9 at −40 and −80 mV, respectively ($P < 0.05$). The filled symbols represent the mean relationship between Ca^{2+} entry and the integrated systolic Ca^{2+} transients at both −40 and −80 mV at the stimulation frequencies indicated. At both holding potentials an increase of stimulation frequency results in a decrease in Ca^{2+} entry via $I_{Ca\text{-}L}$ but a much greater decrease in Ca^{2+} efflux due to the systolic Ca^{2+} transient such that Ca^{2+} efflux due to the systolic Ca^{2+} transient is now less than Ca^{2+} entry. This effect is more pronounced at −80 mV. The role of changing diastolic $[Ca^{2+}]_i$ in maintaining Ca^{2+} flux balance is examined in the right hand panel of Fig. 6*B*. Here the open symbols and regression lines have the same meaning as before at 1 Hz whereas the filled symbols now represent the sum of Ca^{2+} efflux occurring due to *both* the systolic Ca^{2+} transient and the increase of diastolic $[Ca^{2+}]_i$. Under these circumstances, at both holding potentials, as frequency increases the calculated Ca^{2+} efflux now agrees with that required to maintain steady state or Ca^{2+} flux balance conditions as depicted by the regression lines. Figure 7*A* summarizes the mean data showing how Ca^{2+} flux balance is achieved in both experimental conditions (−40 mV, left

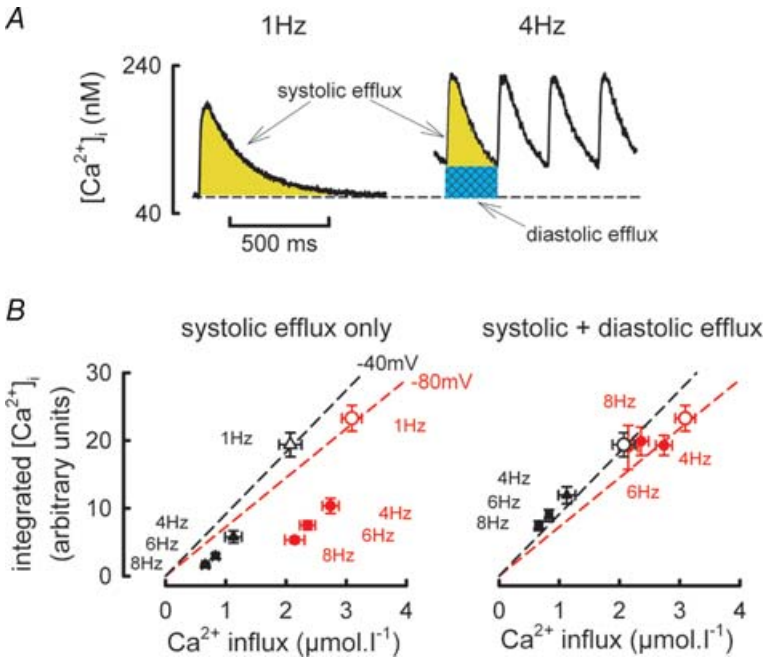

Figure 6. Role for diastolic $[Ca^{2+}]_i$ in maintaining Ca^{2+} flux balance at increased stimulation rates
A, schematic diagram showing calculation of Ca^{2+} efflux due to the systolic Ca^{2+} transient (yellow hatching) and changes in diastolic $[Ca^{2+}]_i$ (cyan hatching) at two stimulation frequencies. *B*, relationship between Ca^{2+} efflux calculated as the integral of the Ca^{2+} transient (ordinate) and Ca^{2+} entry calculated as the integral of $I_{Ca\text{-}L}$ (abscissa). Open symbols represent mean data obtained at a stimulation frequency of 1 Hz and holding potential of −40 mV (black) and −80 mV (red). This data has been fitted with a linear regression (dashed line) passing through the origin. The filled symbols denote Ca^{2+} efflux calculated either from the systolic Ca^{2+} transient alone (left panel) and the total Ca^{2+} efflux calculated as the sum of the systolic Ca^{2+} transient and increase in diastolic $[Ca^{2+}]_i$ (right panel) at the frequencies indicated.

panel; −80 mV, right panel). With increasing stimulation frequency the Ca^{2+} entry per pulse calculated from the integral of $I_{Ca\text{-}L}$ (black) and Ca^{2+} efflux due to the systolic Ca^{2+} transient (red) decrease. However, Ca^{2+} efflux due to the increase in diastolic $[Ca^{2+}]_i$ increases. At −80 mV diastolic $[Ca^{2+}]_i$ contributes 69.3 ± 6% of the total Ca^{2+} efflux at 8 Hz.

Role of β-adrenergic stimulation in the effects of stimulation frequency

In experiments similar to Fig. 1 we have investigated the effect of β-adrenergic stimulation on Ca^{2+} transient amplitude under current clamp conditions. Figure 8*A* shows an experimental time course. Application of 30 nM isoprenaline resulted in a 3.3-fold increase in Ca^{2+} transient amplitude (410 ± 84 to 1201 ± 252 nM at 4 Hz; Fig. 8*B*, $n = 8$, $P < 0.05$). However, increasing stimulation frequency no longer had any effect on Ca^{2+} transient amplitude (6 Hz, 1318 ± 246 nM; 8 Hz, 1159 ± 246 nM; Fig. 8*B*). Nevertheless, diastolic $[Ca^{2+}]_i$ still increases with stimulation frequency in the presence of isoprenaline (4 Hz, 251 ± 22 nM; 6 Hz, 364 ± 19 nM; 8 Hz, 496 ± 51 nM, $P < 0.05$). Figure 8*C* examines if changes in action potential duration are related to the maintenance of the Ca^{2+} transient with increasing stimulation frequency during β-adrenergic stimulation. Initial application of isoprenaline during 4 Hz current clamp stimulation prolonged action potential duration (data not shown), but in the steady state action potential duration was unchanged (APD_{90}, 66 ± 6 ms in control and 72 ± 8 ms in isoprenaline, $P = 0.6$). With increasing stimulation frequency on the other hand, APD_{90} decreased in isoprenaline (6 Hz, 39.1 ± 8 ms; 8 Hz, 25.2 ± 6 ms; $P < 0.05$). Both the rate of decay of the caffeine evoked Ca^{2+} transients (1.8 ± 0.3 *versus* 1.9 ± 0.3 s^{-1}) and the relationship between Na^+–Ca^{2+} exchange current and $[Ca^{2+}]_i$ (slopes −0.199 ± 0.05 *versus* −0.165 ± 0.09, $n = 4$–7) were unaltered by β-adrenergic stimulation. Thus the correction factor for Ca^{2+} removal by PMCA is not altered by β-adrenergic stimulation. Having established this, SR Ca^{2+} content increases in line with Ca^{2+} transient amplitude on application of isoprenaline (4 Hz, control 82.6 ± 15 μmol l^{-1}, isoprenaline, 154 ± 20 μmol l^{-1}; $P < 0.001$, Fig. 8*E*). However, there was no further change in SR Ca^{2+} content with frequency during β-adrenergic stimulation (6 Hz, 169 ± 18 μmol l^{-1}; 8 Hz, 167 ± 21 μmol l^{-1}).

In voltage clamp experiments β-adrenergic stimulation doubled peak $I_{Ca\text{-}L}$ (Fig. 5*A* and *B*, 4 Hz control, 5.7 ± 0.4 pA pF^{-1}; 4 Hz isoprenaline, 12.6 ± 1.8 pA pF^{-1}; $P < 0.005$, $n = 5$–7 cells). As was the case in control conditions (cf. Fig. 3), increasing stimulation frequency decreased the size of the Ca^{2+} transient and peak $I_{Ca\text{-}L}$. When normalized to the respective values at 1 Hz, Ca^{2+} transient amplitude decreased with frequency (4 Hz, 93.2 ± 3; 6 Hz, 69.4 ± 7%; 8 Hz, 53.1 ± 7%) as did peak $I_{Ca\text{-}L}$ (4 Hz, 95.5 ± 1%; 6 Hz, 74 ± 3%; 8 Hz, 40 ± 2%).

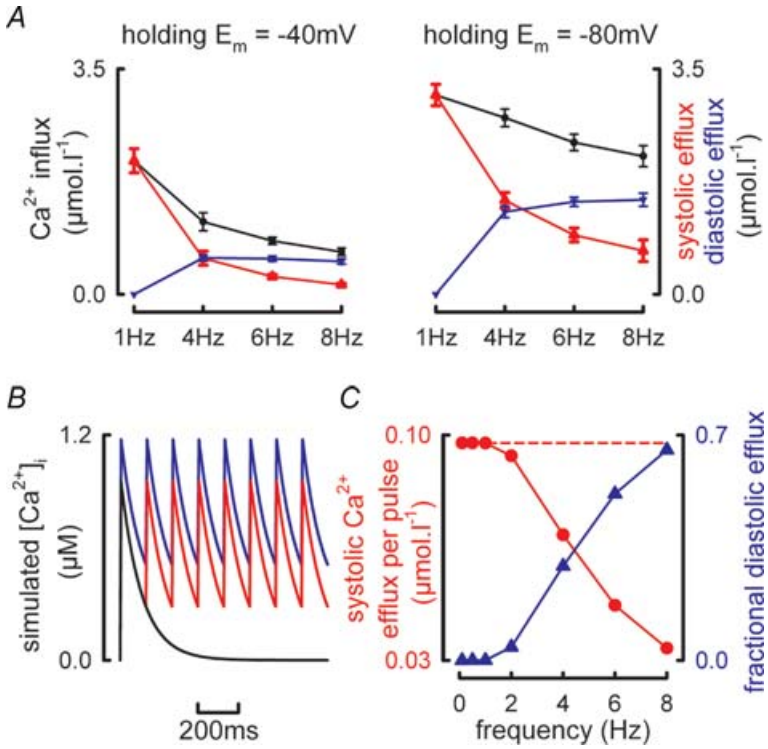

Figure 7. Frequency and voltage dependence of Ca^{2+} influx by $I_{Ca\text{-}L}$ and efflux though systolic and diastolic $[Ca^{2+}]_i$
A, mean data summarizing the frequency dependence of Ca^{2+} entry per pulse via $I_{Ca\text{-}L}$ (black), Ca^{2+} efflux during systole (red) and Ca^{2+} efflux due to changes in diastolic $[Ca^{2+}]_i$ (blue). All changes in Ca^{2+} efflux due to changes in diastolic $[Ca^{2+}]_i$ are referenced to changes in diastolic $[Ca^{2+}]_i$ at a stimulation frequency of 1 Hz. Data obtained at a holding potential of −40 mV (left panel) and −80 mV (right panel). *B*, simulated Ca^{2+} transients delivered at 0.1 Hz (black) and 8 Hz (red and blue) having rate constants of decay of 10 s^{-1} and identical Ca^{2+} influx per pulse. The blue trace shows the increase in diastolic $[Ca^{2+}]_i$ required to balance Ca^{2+} entry when Ca^{2+} efflux due to the systolic Ca^{2+} transient is reduced due to the abbreviated Ca^{2+} transient. *C*, simulation results showing calculated Ca^{2+} efflux obtained by integrating the systolic Ca^{2+} transients in *B* (red symbols) and the fractional contribution made to total Ca^{2+} efflux by changes in diastolic $[Ca^{2+}]_i$ (blue traces). The broken line represents the Ca^{2+} efflux required to match Ca^{2+} influx during the simulated action potential.

The negative $[Ca^{2+}]_i$–frequency relationship still occurred despite SR Ca^{2+} content increasing between 1 and 4 Hz (Fig. 3*B*, lower panel; 1 Hz, 143 ± 9 μmol l^{-1}; 4 Hz, 170 ± 10 μmol l^{-1}; $P < 0.05$) and remaining elevated at the higher frequencies (6 Hz, 171 ± 11 μmol l^{-1}; 8 Hz, 179 ± 14 μmol l^{-1}; n.s.).

Discussion

In this study we have shown that (i) SR Ca^{2+} content increased over the physiological range of stimulation frequencies in the rat, (ii) at higher frequencies Ca^{2+} transient amplitude decreases despite the increase in SR Ca^{2+} content, (iii) lack of recovery of $I_{Ca\text{-}L}$ from inactivation is involved in this decrease of systolic Ca^{2+} phenomenon but is *not* the sole mechanism, (iv) both an increase of diastolic $[Ca^{2+}]_i$ and decrease of $I_{Ca\text{-}L}$ contribute to maintaining Ca^{2+} flux balance, and (v) β-adrenergic stimulation resulted in a frequency-independent increase in Ca^{2+} transient amplitude and SR Ca^{2+} content. To our knowledge this is the first study to systematically determine the complex interplay between $I_{Ca\text{-}L}$ and diastolic $[Ca^{2+}]_i$ in maintaining Ca^{2+} flux balance at appropriate stimulation rates in the rat and during β-adrenergic stimulation. Additionally, we have determined how the physiologically relevant mediator of increases in heart rate, β-adrenergic stimulation modulates the $[Ca^{2+}]_i$–frequency relationship in an SR-independent manner.

Frequency dependent increase in SR Ca^{2+} content

Over the physiological range of stimulation frequencies for the rat, an increase in SR Ca^{2+} content occurred that was paralleled by a frequency-dependent acceleration of decay of $[Ca^{2+}]_i$. This latter observation has been previously reported across a broad range of species and stimulation frequencies (Hussain *et al.* 1997; Antoons *et al.* 2002; Taylor

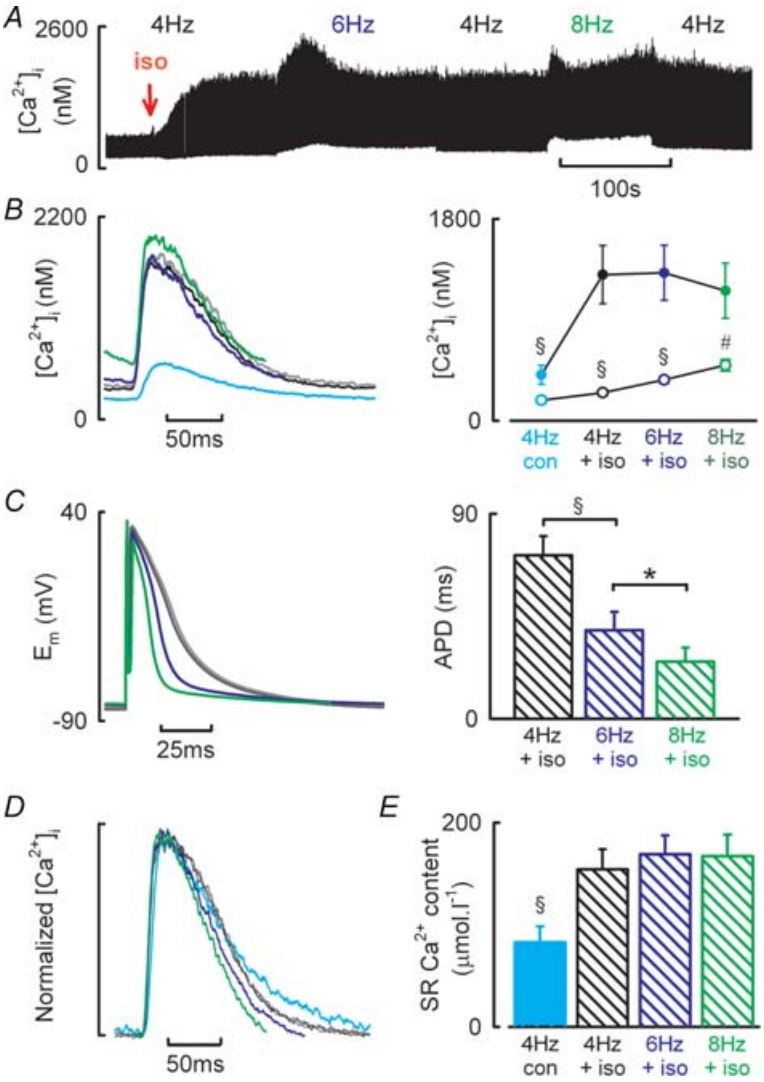

Figure 8. The effect of β-AR stimulation on the Ca^{2+} transient–frequency relationship in isolated rat ventricular myocytes
A, typical experimental time course showing action potential induced changes in $[Ca^{2+}]_i$. Isoprenaline (30 nM) was applied at the time indicated by the downward arrow. Cells were stimulated by applying a 2–4 ms depolarizing current injection at the frequencies of stimulation indicated. *B*, representative Ca^{2+} transients (left) and mean data (right) showing Ca^{2+} transient amplitude (filled symbols) and diastolic $[Ca^{2+}]_i$ (open symbols) obtained at the frequencies indicated. *C*, representative action potentials (left) and mean data summarizing time to 90% repolarization at the stimulation frequencies indicated. *D*, normalized Ca^{2+} transient data illustrating frequency-dependent acceleration of $[Ca^{2+}]_i$ decay. *E*, mean data showing SR Ca^{2+} content measurements obtained following steady-state stimulation at 4 Hz in control conditions (filled bar) or in the presence of 30 nM isoprenaline at the frequencies indicated (hatched bars). *B*–*E* show control 4 Hz (cyan), isoprenaline 4 Hz (black and grey), isoprenaline 6 Hz (blue) and isoprenaline 8 Hz (green). §$P < 0.001$ and #$P < 0.01$ *versus* isoprenaline or previous frequency.

et al. 2004; Zhao *et al.* 2004). The precise mechanisms responsible for the accelerated rate of SERCA mediated Ca^{2+} uptake are complex and were not investigated in the present study. However, we found the SR-dependent rate of $[Ca^{2+}]_i$ decay to be increased with frequency whilst Na^+–Ca^{2+} exchange mediated Ca^{2+} efflux, measured as the relationship between Na^+–Ca^{2+} exchange current and $[Ca^{2+}]_i$, was unaltered. Irrespective of the mechanism that is responsible for the accelerated decay of the systolic Ca^{2+} transient, the enhanced SERCA mediated Ca^{2+} uptake is likely to contribute to the increase in SR Ca^{2+} content with stimulation frequency.

SR Ca^{2+} content is a powerful determinant of systolic Ca^{2+} transient amplitude (Bassani *et al.* 1995; Trafford *et al.* 2000; 2001). Therefore the frequency-dependent increases in SR Ca^{2+} content would be predicted to produce a similar increase in the amplitude of the systolic Ca^{2+} transient. Indeed the lack of a positive force–frequency relationship in rat reported in a number of studies has been attributed to an inability to increase SR Ca^{2+} content further (reviewed in Bers, 2001) although this is clearly not the case in the present study. The present study shows that the relationship between SR Ca^{2+} content and Ca^{2+} transient amplitude is more complex with stimulation frequency increasing both SR Ca^{2+} content and Ca^{2+} transient amplitude at rates between 4 and 6 Hz. However, at higher rates (8 Hz) SR Ca^{2+} content continued to increase whilst Ca^{2+} transient amplitude was reduced.

Role for $I_{Ca\text{-}L}$ in the frequency-dependent response in rat ventricular myocytes

Several studies have demonstrated a use-dependent facilitation of $I_{Ca\text{-}L}$ and suggested that such a phenomenon may underlie the frequency-dependent increase of APD (Fedida *et al.* 1988; Hryshko & Bers, 1990; Fauconnier *et al.* 2003; Guo & Duff, 2003; Guo & Duff, 2006). However, our data and that of one on mouse ventricular myocytes (Antoons *et al.* 2002) finds no evidence for frequency-dependent facilitation of $I_{Ca\text{-}L}$ and shows that peak $I_{Ca\text{-}L}$ decreases with increasing stimulation frequency. As suggested by Antoons *et al.* (2002), such disparate results may result directly from the differences in intracellular Ca^{2+} buffering given that use-dependent facilitation of $I_{Ca\text{-}L}$ is *only* observed under conditions of increased intracellular Ca^{2+} buffering (Fedida *et al.* 1988; Hryshko & Bers, 1990; Fauconnier *et al.* 2003; Guo & Duff, 2003) or at very slow rates of stimulation and non-physiological temperatures (Guo & Duff, 2006).

Under the experimental conditions of voltage clamp control with minimal perturbation of the intracellular milieu (perforated patch with amphotericin-B) the amplitude of the systolic Ca^{2+} transient decreases with increasing stimulation frequency both in control conditions and during β-adrenergic stimulation, an effect that occurs despite SR Ca^{2+} content increasing. The reduction in Ca^{2+} transient amplitude is paralleled by a decrease in peak (trigger) $I_{Ca\text{-}L}$. As suggested by Antoons *et al.* (2002), a likely mechanism for the decrease in peak $I_{Ca\text{-}L}$ with increasing stimulation frequency is incomplete recovery from inactivation. The observation in the present study that the reduction in $I_{Ca\text{-}L}$ with frequency is greater at a holding potential of -40 mV than when a holding potential of -80 mV is used is consistent with a role for incomplete recovery of $I_{Ca\text{-}L}$.

Additionally, the use of appropriate stimulation frequencies for the rat (4–8 Hz) used in this study may further explain the dichotomy between the present data and those of Antoons *et al.* (2002) on the one hand with those where use-dependent facilitation of $I_{Ca\text{-}L}$ is observed, e.g. using slow rates of stimulation (0.05–2 Hz) (Guo & Duff, 2006). Under the conditions of our experiments the time available for $I_{Ca\text{-}L}$ recovery from inactivation decreases with increasing stimulation frequency due to the combined effects of the increased rate and longer APD at higher rates. Indeed at intervals observed at the present rates of stimulation (75–200 ms), a number of studies using paired pulse protocols to investigate $I_{Ca\text{-}L}$ recovery from inactivation show that $I_{Ca\text{-}L}$ availability is markedly reduced at short intervals following the preceding depolarization (Li *et al.* 1999; Altamirano & Bers, 2007). Thus at physiologically relevant rates of stimulation for the rat, or indeed at increased rates of stimulation in heart disease where action potential duration is prolonged (Sipido *et al.* 1998; Díaz *et al.* 2004), the decrease in $I_{Ca\text{-}L}$ availability is likely to be an important factor responsible for the flat or negative force–frequency relationships observed.

However, the data of Fig. 4 indicate that, under voltage clamp conditions, reductions in $I_{Ca\text{-}L}$ are not the sole mechanism responsible for the decrease in Ca^{2+} transient amplitude with increasing stimulation frequency. In these experiments normalization of $I_{Ca\text{-}L}$ achieved by reducing the amplitude of the voltage clamp step resulted in a significantly smaller decrease in Ca^{2+} transient amplitude than similar decreases in $I_{Ca\text{-}L}$ achieved through increased stimulation frequency. Changes in SR Ca^{2+} content are not responsible for this phenomenon since the SR Ca^{2+} content at the stimulation frequency at which the reduced test step is delivered is *less* than that when $I_{Ca\text{-}L}$ is reduced by the higher stimulation frequency (i.e. Fig. 2). In accordance with previous speculation (Antoons *et al.* 2002), one mechanism that may be involved in this phenomenon involves a role for recovery of the RyR from inactivation, alternatively known as RyR refractoriness (Sham *et al.* 1998; DelPrinciple *et al.* 1999). Whilst we have not established a direct role for RyR refractoriness in the paradoxically smaller Ca^{2+} transients observed when $I_{Ca\text{-}L}$ is reduced by increased stimulation frequency

the apparent absolute refractory period of the RyR of ~30–60 ms, measured as the minimum time between successive Ca^{2+} sparks, approximates closely to the inter-stimulus intervals used in these experiments and leaves open the possibility that such a phenomenon may be important at high stimulation rates (Sham *et al.* 1998; Sobie *et al.* 2005).

The importance of changes in diastolic $[Ca^{2+}]_i$

Under all of the experimental conditions in the present study an increase in stimulation frequency was associated with elevated diastolic $[Ca^{2+}]_i$. Similar observations have been observed by others (Layland & Kentish, 1999; Antoons *et al.* 2002), but in these studies the role for the increased diastolic $[Ca^{2+}]_i$ in maintaining cellular Ca^{2+} flux balance was not determined. Over the contractile cycle, in order for Ca^{2+} flux balance to be achieved, the amount of Ca^{2+} entering the cell via $I_{Ca\text{-}L}$ must be balanced by an equal loss largely by the Na^+–Ca^{2+} exchanger. The magnitude of the Ca^{2+} efflux will in turn depend both on the properties of the Na^+–Ca^{2+} exchanger, which we find is unaltered by frequency (Fig. 2), and the size and duration (i.e. the integral) of the systolic Ca^{2+} transient. The combined effects of increasing stimulation frequency and the frequency-dependent acceleration of decay of the systolic Ca^{2+} transient will result in a reduced opportunity for Ca^{2+} efflux during the systolic Ca^{2+} transient. There are three possible ways in which the cell could maintain Ca^{2+} flux balance under these circumstances: (i) increasing the amplitude of the systolic Ca^{2+} transient, (ii) reducing Ca^{2+} entry via $I_{Ca\text{-}L}$, and (iii) increasing Ca^{2+} efflux by elevating diastolic $[Ca^{2+}]_i$. Whilst a positive force–frequency relationship occurs in many species (Kurihara & Sakai, 1985; Pieske *et al.* 1999; Maier *et al.* 2000), our data demonstrates that under voltage clamp the amplitude of the systolic Ca^{2+} transient in the rat *decreases* with increased stimulation frequency (Fig. 3). Additionally, whilst the total Ca^{2+} entry via $I_{Ca\text{-}L}$ decreases with rate there is a disproportionately greater fall in the integrated systolic Ca^{2+} transient (i.e. Ca^{2+} efflux due to the systolic transient, Figs 6*B* and 7*A*). However, under these circumstances, the increase in diastolic $[Ca^{2+}]_i$ and the Ca^{2+} efflux that this promotes re-establishes Ca^{2+} flux balance, thus highlighting the importance that changes in diastolic $[Ca^{2+}]_i$ play in maintaining steady state conditions.

The importance of the changes in diastolic $[Ca^{2+}]_i$ can be modelled. For the simple simulation presented in Fig. 7*B*, two sets of 'systolic Ca^{2+} transients' have been generated using a single exponential decay function ($[Ca^{2+}]_i = 1 \times e^{-kt}$) each with a rate constant of decay (k) of 10 s^{-1} (mean rate constant of decay under voltage clamp conditions at 1 Hz, 10.7 ± 0.7 s^{-1}). The first (black) at a slow rate of stimulation (0.1 Hz) where $[Ca^{2+}]_i$ decays fully, and a second (red) at a fast rate of stimulation (8 Hz) where time (t) is reset to 0 and the above function is repeated every 125 ms. If we assume under these simplified simulated circumstances (i) Ca^{2+} entry per pulse remains constant and (ii) Ca^{2+} efflux is proportional to $[Ca^{2+}]_i$ then at increasing stimulation frequencies the Ca^{2+} efflux per pulse will decrease as a direct result of the lack of recovery of the systolic Ca^{2+} transient (Fig. 7*C*, red symbols). The inequality between Ca^{2+} entry and efflux can be compensated by a 'DC' increase in $[Ca^{2+}]_i$ as shown by the blue trace in Fig. 7*B*. Figure 7*C* illustrates how the increase in diastolic $[Ca^{2+}]_i$ contributes to maintaining Ca^{2+} flux balance with increasing stimulation frequency. Whilst the above simulation takes no account of actual changes in SERCA activity nor Ca^{2+} entry via $I_{Ca\text{-}L}$, it does demonstrate the important role played by changes in diastolic $[Ca^{2+}]_i$. It should, however, be noted that, while the increase of diastolic $[Ca^{2+}]_i$ may be useful in maintaining flux balance, it will also tend to produce diastolic contraction and, if excessive, may impair ventricular filling.

Relationship between $[Ca^{2+}]_i$ and frequency during β-adrenergic stimulation

It is established that β-adrenergic stimulation results in positive inotropic, lusitropic and chronotropic responses *in vivo* and increases the amplitude and rate of decay of the systolic Ca^{2+} transient in isolated cardiac myocytes (for review see Bers, 2001). These effects occur through a number of mechanisms of which PKA-dependent phosphorylation of PLB, the L-type Ca^{2+} channel and troponin I are all involved. Given the broad range of cellular targets and the key role that β-adrenergic stimulation plays in increasing heart rate *in vivo*, we sought to determine if it modulates the $[Ca^{2+}]_i$–frequency relationship in isolated myocytes. Under current clamp conditions, β-adrenergic stimulation increased the amplitude of the systolic Ca^{2+} transient; however, there was no longer any frequency dependence of Ca^{2+} transient amplitude and this was paralleled by no frequency-dependent change in SR Ca^{2+} content (measured following current clamp stimulation). The above data obtained following current clamp stimulation may have arisen through β-adrenergic stimulation resulting in maximal stimulation of PLB and thus SERCA mediated Ca^{2+} uptake and therefore no change in SR Ca^{2+} content with stimulation rate. Coupled to this, under conditions of high SR Ca^{2+} load, the gain of excitation–contraction coupling is also very high (Bassani *et al.* 1995; Trafford *et al.* 2001; Ginsburg & Bers, 2004). Thus, changes in Ca^{2+} entry during the action potential become redundant as SR fractional release is maximal in response to the initial Ca^{2+} entry.

However, a subtly different picture emerges when the experiments are repeated under voltage clamp control to specifically investigate the role of $I_{Ca\text{-}L}$ and SR Ca^{2+} content in the frequency–$[Ca^{2+}]_i$ relationship during β-adrenergic stimulation. Under these circumstances, both SR Ca^{2+} content and Ca^{2+} transient amplitude display frequency-dependent alterations but in the opposite directions, i.e. Ca^{2+} transient amplitude decreases and SR Ca^{2+} content increases with frequency. These data are perhaps initially surprising given the known effects of PKA mediated phosphorylation on cardiac excitation–contraction coupling (ECC) and the expectation that the gain of ECC should increase (Bers, 2001). This latter point is difficult to examine experimentally given the dual effects of β-adrenergic stimulation increasing trigger $I_{Ca\text{-}L}$ and potentially SR Ca^{2+} content. However, in a study where SR Ca^{2+} content and $I_{Ca\text{-}L}$ were very carefully controlled, β-adrenergic stimulation was found not to alter ECC gain rather the SR Ca^{2+} release rate (Ginsburg & Bers, 2004).

Finally, it is worth considering the effects of frequency-dependent acceleration of relaxation (by either PKA or CAMKII) on cellular Ca^{2+} flux balance. Such an effect has the advantage that the faster rate of decay of the Ca^{2+} transient will help with diastolic relaxation and therefore ventricular filling. However, the abbreviation of the Ca^{2+} transient will decrease Ca^{2+} efflux and thus exacerbate the problem of obtaining sufficient Ca^{2+} efflux at higher heart rates. It may be that in species where the SR is *not* operating near maximal capacity the increased SERCA mediated Ca^{2+} uptake increases SR Ca^{2+} content and thus the amplitude of the systolic Ca^{2+} transient and thereby increases Ca^{2+} efflux to match influx with a decreased need to increase diastolic $[Ca^{2+}]_i$.

Conclusions

We have shown that in isolated rat ventricular myocytes and experimental conditions designed to be as physiologically relevant as possible using an *in vitro* experimental system (rates of stimulation, temperature and minimal perturbation of the intracellular milieu) there is a complex relationship between stimulation frequency, SR Ca^{2+} content and the amplitude of the systolic Ca^{2+} transient. We find *no* evidence for facilitation of $I_{Ca\text{-}L}$ with increasing stimulation frequency and highlight the important role that diastolic $[Ca^{2+}]_i$ has for maintaining a balance between Ca^{2+} influx and efflux during the contractile cycle. Importantly, when the role of reductions of $I_{Ca\text{-}L}$ in the negative Ca^{2+} transient–frequency relationship was investigated we found that another factor is also involved in this phenomenon. We speculate that this may be refractoriness of the RyR, an effect that would become more important at higher stimulation frequencies. The physiological accelerator of heart rate, β-adrenergic stimulation, flattened the action potential induced Ca^{2+} transient–frequency relationship and is consistent with β-adrenergic stimulation producing a situation where SR Ca^{2+} release becomes maximal in response to the initial trigger Ca^{2+} entry via $I_{Ca\text{-}L}$.

In summary, our data demonstrates that the mechanisms underlying the Ca^{2+} transient–frequency relationship in cardiac muscle are complex. Comprehending how this relationship is altered in disease situations would require not only consideration of SR Ca^{2+} content, $I_{Ca\text{-}L}$ and diastolic $[Ca^{2+}]_i$, but also a possible role for refractoriness of the SR Ca^{2+} release channel, or RyR, and this in itself may become a more important consideration during higher rates of stimulation.

References

Altamirano J & Bers DM (2007). Effect of intracellular Ca^{2+} and action potential duration on L-type Ca^{2+} channel inactivation and recovery from inactivation in rabbit cardiac myocytes. *Am J Physiol Heart Circ Physiol* **293**, H563–H573.

Antoons G, Mubagwa K, Nevelsteen I & Sipido KR (2002). Mechanisms underlying the frequency dependence of contraction and Ca^{2+} transients in mouse ventricular myocytes. *J Physiol* **543**, 889–898.

Bassani JWM, Yuan W & Bers DM (1995). Fractional SR Ca release is regulated by trigger Ca and SR Ca content in cardiac myocytes. *Am J Physiol Cell Physiol* **268**, C1313–C1329.

Bers DM (2001). *Excitation–Contraction Coupling and Cardiac Contractile Force*, 2nd edn. Kluwer Academic Publishers, Dordrecht/Boston/London.

Bouchard RA & Bose D (1989). Analysis of the interval-force relationship in rat and canine ventricular myocardium. *Am J Physiol Heart Circ Physiol* **257**, H2036–H2047.

DelPrinciple F, Egger M & Niggli E (1999). Calcium signalling in cardiac muscle: refractoriness revealed by coherent activation. *Nat Cell Biol* **1**, 323–329.

Díaz ME, Graham HK & Trafford AW (2004). Enhanced sarcolemmal Ca^{2+} efflux reduces sarcoplasmic reticulum Ca^{2+} content and systolic Ca^{2+} in cardiac hypertrophy. *Cardiovasc Res* **62**, 538–547.

Dibb KM, Rueckschloss U, Eisner DA, Isenberg G & Trafford AW (2004). Mechanisms underlying enhanced cardiac excitation contraction coupling observed in the senescent sheep myocardium. *J Mol Cell Cardiol* **37**, 1171–1181.

Eisner DA, Trafford AW, Díaz ME, Overend CL & O'Neill SC (1998). The control of Ca release from the cardiac sarcoplasmic reticulum: regulation versus autoregulation. *Cardiovasc Res* **38**, 589–604.

Fauconnier J, Bedut S, Le Guennec JY, Babuty D & Richard S (2003). Ca^{2+} current-mediated regulation of action potential by pacing rate in rat ventricular myocytes. *Cardiovasc Res* **57**, 670–680.

Fedida D, Noble D & Spindler AJ (1988). Use-dependent reduction and facilitation of Ca^{2+} current in guinea-pig myocytes. *J Physiol* **405**, 439–460.

Ginsburg KS & Bers DM (2004). Modulation of excitation-contraction coupling by isoproterenol in cardiomyocytes with controlled SR Ca load and I_{Ca} trigger. *J Physiol* **556**, 463–480.

Guo J & Duff HJ (2003). Inactivation of $I_{Ca\text{-}L}$ is the major determinant of use-dependent facilitation in rat cardiomyocytes. *J Physiol* **547**, 797–805.

Guo J & Duff HJ (2006). Calmodulin kinase II accelerates L-type Ca^{2+} current recovery from inactivation and compensates for the direct inhibitory effect of $[Ca^{2+}]_i$ in rat ventricular myocytes. *J Physiol* **574**, 509–518.

Hryshko LV & Bers DM (1990). Ca current facilitation during post-rest recovery depends on Ca entry. *Am J Physiol Heart Circ Physiol* **259**, H951–H961.

Hussain M, Drago GA, Colyer J & Orchard CH (1997). Rate-dependent abbreviation of Ca^{2+} transient in rat heart is independent of phospholamban phosphorylation. *Am J Physiol Heart Circ Physiol* **273**, H695–H706.

Ito K, Yan X, Tajima M, Su Z, Barry WH & Lorell BH (2000). Contractile reserve and intracellular calcium regulation in mouse myocytes from normal and hypertrophied failing hearts. *Circ Res* **87**, 588–595.

Janssen PM, Stull LB & Marban E (2002). Myofilament properties comprise the rate-limiting step for cardiac relaxation at body temperature in the rat. *Am J Physiol Heart Circ Physiol* **282**, H499–H507.

Kassiri Z, Myers R, Kaprielian R, Banijamali HS & Backx PH (2000). Rate-dependent changes of twitch force duration in rat cardiac trabeculae: a property of the contractile system. *J Physiol* **524**, 221–231.

Kurihara S & Sakai T (1985). Effects of rapid cooling on mechanical and electrical responses in ventricular muscle of guinea-pig. *J Physiol* **361**, 361–378.

Layland J & Kentish JC (1999). Positive force- and $[Ca^{2+}]_i$-frequency relationships in rat ventricular trabeculae at physiological frequencies. *Am J Physiol Heart Circ Physiol* **276**, H9–H18.

Li GR, Yang B, Feng J, Bosch RF, Carrier M & Nattel S (1999). Transmembrane I_{Ca} contributes to rate-dependent changes of action potentials in human ventricular myocytes. *Am J Physiol Heart Circ Physiol* **276**, H98–H106.

Maier LS, Bers DM & Pieske B (2000). Differences in Ca^{2+}-handling and sarcoplasmic reticulum Ca^{2+}-content in isolated rat and rabbit myocardium. *J Mol Cell Cardiol* **32**, 2249–2258.

Picht E, Desantiago J, Huke S, Kaetzel MA, Dedman JR & Bers DM (2007). CaMKII inhibition targeted to the sarcoplasmic reticulum inhibits frequency-dependent acceleration of relaxation and Ca^{2+} current facilitation. *J Mol Cell Cardiol* **42**, 196–205.

Pieske B, Maier LS, Bers DM & Hasenfuss G (1999). Ca^{2+} handling and sarcoplasmic reticulum Ca^{2+} content in isolated failing and nonfailing human myocardium. *Circ Res* **85**, 38–46.

Sham JSK, Song L-S, Chen Y, Deng L-H, Stern MD, Lakatta EG & Cheng H (1998). Termination of Ca^{2+} release by a local inactivation of ryanodine receptors in cardiac myocytes. *Proc Natl Acad Sci U S A* **95**, 15096–15101.

Sipido KR, Stankovicova T, Flameng W, Vanhaecke J & Verdonck F (1998). Frequency dependence of Ca^{2+} release from the sarcoplasmic reticulum in human ventricular myocytes from end-stage heart failure. *Cardiovasc Res* **37**, 478–488.

Sobie EA, Song LS & Lederer WJ (2005). Local recovery of Ca^{2+} release in rat ventricular myocytes. *J Physiol* **565**, 441–447.

Taylor DG, Parilak LD, LeWinter MM & Knot HJ (2004). Quantification of the rat left ventricle force and Ca^{2+}-frequency relationships: similarities to dog and human. *Cardiovasc Res* **61**, 77–86.

Trafford AW, Díaz ME & Eisner DA (1998). Ca-activated chloride current and Na-Ca exchange have different timecourses during sarcoplasmic reticulum Ca release in ferret ventricular myocytes. *Pflugers Arch* **435**, 743–745.

Trafford AW, Díaz ME & Eisner DA (2001). Coordinated control of cell Ca^{2+} loading and triggered release from the sarcoplasmic reticulum underlies the rapid inotropic response to increased L-type Ca^{2+} current. *Circ Res* **88**, 195–201.

Trafford AW, Díaz ME, Negretti N & Eisner DA (1997). Enhanced calcium current and decreased calcium efflux restore sarcoplasmic reticulum Ca content following depletion. *Circ Res* **81**, 477–484.

Trafford AW, Díaz ME, Sibbring GC & Eisner DA (2000). Modulation of CICR has no maintained effect on systolic Ca^{2+}: simultaneous measurements of sarcoplasmic reticulum and sarcolemmal Ca^{2+} fluxes in rat ventricular myocytes. *J Physiol* **522**, 259–270.

Varro A, Negretti N, Hester SB & Eisner DA (1993). An estimate of the calcium content of the sarcoplasmic reticulum in rat ventricular myocytes. *Pflugers Arch* **423**, 158–160.

Zhao W, Uehara Y, Chu G, Song Q, Qian J, Young K & Kranias EG (2004). Threonine-17 phosphorylation of phospholamban: a key determinant of frequency-dependent increase of cardiac contractility. *J Mol Cell Cardiol* **37**, 607–612.

Acknowledgements

This work was funded by The British Heart Foundation.